Ab initio study of hydrogenation effects in amorphous silicon carbide

Fabio Finocchi*
Centre Européen de Calcul Atomique et Moléculaire (CECAM), École Normale Superieure, Aile LR5, 46 Allée d'Italie, 69364 Lyon Cedex 07, France

Giulia Galli
Institut Romand de Recherche Numérique en Physique des Matériaux (IRRMA), IN-Ecublens, 1015 Lausanne, Switzerland
(Received 22 April 1994)

We propose a structural model of hydrogenated amorphous silicon carbide (*a*-SiC:H) at stoichiometric composition and low H content, based on the results of *ab initio* molecular-dynamics simulations. As found for *a*-SiC, the system has a complex structure which cannot be described as a distorted crystalline phase. Nevertheless, the degree of chemical order is larger in the hydrogenated network than in the pure network. H binds to both C and Si. H bound to C gives rise to sp^3 bonded monohydrated sites, thus favoring the formation of a tetrahedral network. H bound to Si forms diverse bonding configurations where weak and strong bonds can be identified. These results are in agreement with recent experiments. Furthermore, our findings for the evolution of Si-H and C-H bonding as a function of temperature are consistent with recent measurements of H desorption from Si-C alloys. Finally, we suggest an interpretation of x-ray and neutron-diffraction data based on analyses of several total distribution functions.

I. INTRODUCTION

The technological importance of hydrogenated amorphous silicon carbide films (*a*-SiC:H) in the fabrication of photovoltaic devices, solar cells, and hard coatings has recently inspired various experimental investigations of these alloys.[1] It is now well established that the short-range order of *a*-SiC:H films depends on their hydrogen content;[2] there is also general agreement upon the role of H in increasing the ratio of heteronuclear to homonuclear bonds, i.e., in enhancing chemical order in Si-C alloys. For example, dilution of methane-silane mixtures with molecular hydrogen during the growth of *a*-SiC has been found to promote chemical order in plasma-enhanced deposited samples,[3,4] and to favor fourfold coordinated C sites.[5]

However, a comprehensive picture of hydrogenation effects in *a*-SiC is lacking; in particular, whether H is more likely to bind to Si than to C, and the specific bonding configurations induced by the presence of H are still open questions. An increase of C concentration in Si-C alloys has been correlated to an increase of H trapping during growth,[6] which may be an indication of H being more likely bound to C than to Si in *a*-SiC:H. On the other hand, H bound to Si has been detected in infrared (IR) absorption experiments[7] of a-$Si_{1-x}C_x$:H, for a wide range of carbon concentrations ($0.1 < x < 0.7$), and the presence of Si-H bonds probed by recent neutron scattering experiments[4] on silicon rich alloys.

A long-standing subject of controversy concerns the degree of chemical order in *a*-SiC:H.[1] The results of different experiments using the same techniques, e.g., x-ray photoemission spectroscopy (XPS) and extended x-ray absorption fine structure spectroscopy (EXAFS), has led to establishing different ratios of homonuclear to heteronuclear bonds in alloys with approximately the same H content. This may be partially due to genuine structural differences between samples prepared under different conditions. However, the controversy about chemical order arises mainly from difficulties in the interpretation of experiment. For example, it has been pointed out[8] that both chemically ordered and random distribution models can well reproduce core level shifts measured by XPS as a function of the alloy composition. Furthermore, incongruous ratios of Si-Si to Si-C bonds have been determined from the analysis of EXAFS signals measured by different groups[9,10] for samples prepared under similar conditions.

In order to investigate the issues of chemical order and H bonding in *a*-SiC:H we performed first-principles molecular dynamics (MD) simulations[11] of an *a*-SiC:H alloy at stoichiometric composition, containing about 20% hydrogen. To our knowledge, this is the first theoretical study of the structural properties of hydrogenated *a*-SiC. The presence of covalent bonds and of species with different chemical behaviors such as Si, C, and H calls for a quantum mechanical description of the atomic interactions. In our simulations interatomic forces were derived at each step by quantum mechanical calculations, based on density functional theory, within the local density approximation. This approach[11] has already proved powerful in predicting a variety of properties of amorphous semiconducting materials, such as of both pure and hydrogenated *a*-Si (Ref. 12) and *a*-C (Ref. 13) and of *a*-SiC.[14]

The results of our simulations allow one to characterize the bonding configurations of *each* atomic species and to elucidate the role of H in determining the microscopic structure of an *a*-SiC alloy; furthermore, they provide

an interpretation of x-ray and neutron diffraction experiments based on the analysis of *total* correlation functions.

II. COMPUTATIONAL METHOD

We considered an atomic H concentration (n_H), 19%, at the bottom range of concentrations in so-called high quality samples, used in photovoltaic devices, and we initially fixed the film density ρ at 3.18 gr/cm^3, close to the density of cubic c-SiC. In our simulations we used a supercell containing 32 Si, 32 C, and 12 H atoms, with simple cubic periodic boundary conditions. The interaction between ionic cores and valence electrons was described by norm-conserving pseudopotentials[16] including s and $(s + p)$ nonlocality for C and Si, respectively. The pure coulombic potential was used for H. The electronic wave functions and the charge density were expanded in plane waves with energy cutoffs (E_{cut}) of 35 Ry and 140 Ry, respectively. The supercell Brillouin zone was sampled only with the Γ point. Calculations of the equilibrium volume and of the band structure of c-SiC and of the bond lengths and vibrational frequencies of the molecules SiH_4 and CH_4 were performed in order to test our choices for the pseudopotential and for E_{cut}. Our results[17] are in good agreement with existing calculations and with experiments.

An a-SiC:H network was generated by rapid quenching from a liquid at $T \simeq 4000$ K. A SiC liquid state was first obtained, by heating up to melting a crystalline lattice in the zinc-blende structure; randomly placed H atoms were then added to the system, and the whole sample equilibrated for about 1 ps. The system was brought to 500 K with a cooling rate $\dot{T} \simeq -2 \times 10^{15}$ K/s (where the dot indicates time derivatives). After a short run at room temperature, it was heated up again to about 1400 K, and cooled down at room temperature with $\dot{T} \simeq -0.7 \times 10^{15}$ K/ps. Throughout the whole annealing procedure we computed the pressure acting on the system and the supercell volume was rescaled so that the density at the end of the annealing cycle would be within 1–2% of its equilibrium value. Statistical properties were computed at $T = 260$ K, over a 1.5 ps run.

III. RESULTS AND DISCUSSION

Analyses of the ionic trajectories obtained in our simulation show that the computer generated sample is a highly distorted tetrahedral network with both homonuclear and heteronuclear bonds, which cannot be described as a distorted crystalline phase. These results are consistent with those of electron diffraction measurements[15] and with recent EXAFS data.[9] The relative proportions of C and Si bonds are $N_{C-C}/N_{C-Si} \simeq 0.5$, and $N_{Si-Si}/N_{C-Si} \simeq 0.6$, where N_{I-J} indicates the number of bonds between species I and J. The number of heteronuclear bonds is more abundant than in a computer generated unhydrogenated network,[14] revealing a moderate tendency towards chemical order. H is found to bind to both C and Si, in agreement with the indications of recent experiments.[20,21] Carbon has a total coordination very close to four (3.97), larger than in a-SiC (3.85). Indeed, only one threefold coordinated C site is found in our sample. The increase in C coordination is due to the presence of H, which binds to carbons bonded to three other atoms (either C or Si). This gives rise to fourfold coordinated $C^{(4)}$-H units,[18] which are the only kind of hydrogenated C sites found in our sample. The C-H bond distance (1.12 Å), as indicated by the position of the intense first peak of the correlation function g_{C-H} shown in Fig. 1 (lower panel), is very close to the corresponding bond length calculated (with the same E_{cut}) for the CH_4 molecule. The $C^{(4)}$-C bond length, larger than in pure a-SiC, is closer to the diamond than to the graphite first-neighbor distance. As far as bond angles are concerned, we note that both Si-C-H and C-C-H angular distributions have a sharp peak around 109°. We can therefore conclude that $C^{(4)}$-H units are sp^3 bonded, tetrahedral sites, in agreement with photoconductivity[2] and electron paramagnetic resonance measurements.[19] The bonding properties of protonate C are remarkably similar to those of C sites bonded to H found in a-C:H[13].

Contrary to hydrogenated carbons, C not bound to H gives rise to distorted tetrahedral configurations. The average C-Si first-neighbor distance (1.87 Å) is close to the corresponding distance computed for cubic c-SiC (1.89 Å) and the position of the second peak of both g_{C-C} and g_{Si-Si} are very close to the second-neighbor distances in cubic c-SiC (3.08 Å). However, both C-C-C and C-Si-C angular distributions show two structures at 109° and at 120°, indicating that unhydrogenated C sites can have bonding configurations with hybridization intermediate between sp^3 and sp^2.

Si-Si and Si-H bonds are more complex to characterize than their carbon counterparts. Si total coordination is larger than four ($\simeq 4.4$); indeed, a large number of fivefold coordinated Si atoms ($Si^{(5)}$) is present in our computer generated network. This large amount of $Si^{(5)}$ could be partially an artifact of the small size of the MD cell and of the fast quenching rates. In our simulation, at the end of the second annealing cycle we find a smaller number of $Si^{(5)}$ sites than after the first cycle, together with better defined peaks in g_{Si-H} and g_{Si-Si} correlation functions. Nevertheless, a concentration of fivefold Si sites bigger than the one found, e.g., in a-Si and a-Si:H

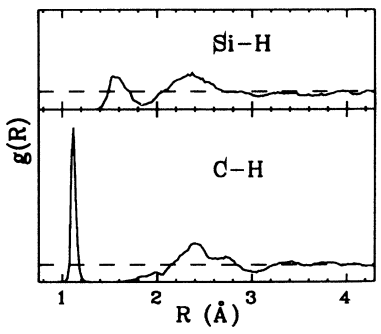

FIG. 1. Calculated C-H (lower panel) and Si-H (top panel) partial distribution functions.

is expected to be a genuine feature of a-SiC alloys prepared by quenching, and to possibly arise from the large difference between the energies of C-C, Si-C, and Si-Si bonds.

The g_{Si-H} correlation function, shown in Fig. 1 (top panel), has a broad first maximum at 1.54 Å , to be contrasted with the intense first peak of g_{C-H}. The spreadout of Si-H bond distances indicates that different types of Si-H bonding configurations are present in the network. We find both $Si^{(4)}$-H and $Si^{(5)}$-H units in our sample. In $Si^{(4)}$-H sites, the Si-H bond distance is very close to that of silane (1.50 Å), whereas in $Si^{(5)}$-H units the Si-H bond length is approximately 1.6 Å. Long (weak) Si-H bonds give rise to Si-H-Si bridge configurations with bond angles of the order of 130°. The occurrence of Si-H-Si bridges, which becomes more probable as T is lowered during the annealing cycle, could be directly related to the presence of $Si^{(5)}$. It might be a consequence of the conversion between $Si^{(5)}$ defects and weak Si-H bonds similar to that suggested to take place in a-Si:H,[22] according to the path $Si^{(5)}$-H + $Si^{(4)}$-$Si^{(5)} \rightarrow$ $Si^{(4)}$ + $Si^{(4)}$-H-$Si^{(5)}$, as a function of decreasing T.

In our simulation we did not find any tendency of H atoms to be clustered, contrary to a-Si:H[12] but similar to a-C:H[13]; we observed, however, the formation of a H_2 molecule during the annealing cycle, which turned out to be stable also at room temperature.

As T is raised from 300 K to about 1400 K in our second annealing cycle, g_{Si-H} becomes less structured and the intensity of its first peak becomes very close to one, inferior to that of the second maximum. On the contrary, no significant change in g_{C-H} is observed: its sharp first peak remains very similar to that shown in Fig. 1, over a wide T range. These results are consistent with those of recent IR measurements[20,21] on SiC alloys, performed as a function of increasing T: H is found to desorb first from Si; it can then bind to C if unprotonate C sites are present in the alloy, and finally leave the sample at a temperature much larger than that needed to break Si-H bonds.

A direct comparison with data from x-ray (XR) or neutron diffraction (ND) experiments is not yet possible, since at present there are no measurements for films with the same composition and H content as our computer generated network. However, it is interesting to discuss how the results of our simulation are to be compared to those of these experiments, and how diffraction techniques are able to discriminate among the many bonding configurations found in a-SiC:H. In order to do so, we analyze total distribution functions (DF). In the top panel of Fig. 2 we display the bare DF

$$J_B(R) = 4\pi R^2 n G_B(R) = 4\pi R^2 n \sum_{I,J} c_I c_J g_I J(R) \quad (1)$$

obtained from the partial correlation functions $g_{IJ}(R)$ computed in our simulation. n denotes the average *number* density and c_I the atomic concentration of species I. The sum extends to all of the atomic species. The peak positions of $G_B(R)$ are given in Table I, where they are associated with specific bond lengths according to the positions of the $g_{IJ}(R)$ maxima.[23] The middle panel of Fig.

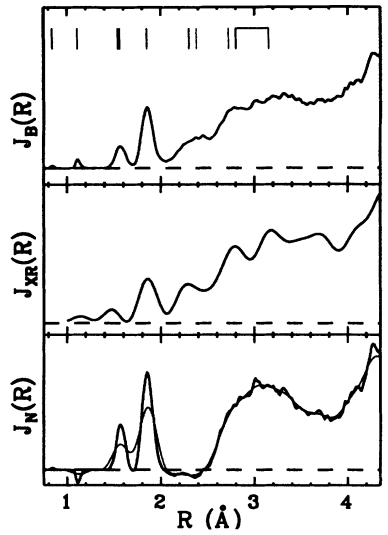

FIG. 2. Bare total distribution function J_B (upper panel) and total distribution functions to be compared with x-ray, J_{XR} (middle panel) and neutron diffraction J_N (lower panel) data (see text). In the upper panel vertical bars indicate the position of the peaks specified in Table I. In the lower panel the thick and thin lines correspond to bare and convoluted data (q_{max} = 30 $Å^{-1}$), respectively.

TABLE I. The first column gives the position ($\bar{R}$) of the mth maximum of the partial distribution functions $g_{IJ}(R)$. The value of m and the type of atomic species I, J (C, Si, H) are given in columns 2 and 3, respectively. The intensities of the maxima of $G_B(R) = \sum_{I,J} c_I c_J g_{IJ}(R)$ (see text), defined as $W = c_I c_J (2 - \delta_{IJ}) g_{IJ}(\bar{R})$, are given in column 4. The maxima of $J_B(R)$ corresponding to those of $G_B(R)$ listed here are marked in Fig. 2 (upper panel). Distances are indicative values (Ref. 23).

$\bar{R}$ (Å)	m	I-J	W
0.84	1	H-H	0.5
1.12	1	H-C	1.2
1.54	1	H-Si	0.2
1.56	1	C-C	1.3
1.85	1	C-Si	3.0
2.30	1	Si-Si	0.3
2.38	2	H-C + H-Si	0.3 + 0.3
2.72	2	C-Si	0.5
2.8	2	C-C + Si-Si	0.3 + 0.3
3.0	3	C-C + Si-Si	0.3 + 0.3
3.1	4	C-C + Si-Si	0.3 + 0.3

2 shows the DF $J_{XR}(R)$, obtained as Fourier transform (FT) of

$$S(q) = \frac{\sum_{I,J} f_I(q) f_J(q) S_{IJ}(q)}{\sum_I f_I^2(q)}. \quad (2)$$

Here $f_I(q)$ is the atomic XR form factor for species I and $S_{IJ}(q)$ the partial structure factors computed as for pure a-SiC.[14] J_{XR} can be compared directly to the FT of measured scattered XR intensities. The peak positions of the calculated J_{XR} at $R = 1.49$, 1.87, and 2.30 Å are in agreement with those of the corresponding DF reported in Ref. 24, for films with 0.3 and 0.7% C content. A comparison between $J_B(R)$ and $J_{XR}(R)$ shows that the most intense maxima of $J_{XR}(R)$ are associated with Si-C and Si-Si first- and second-neighbor distances. Structures arising from C-C bonds and from C-H or Si-H bonds appear only as blurred maxima or weak shoulders in J_{XR}. Indeed, in XR elastic scattering Si is weighted more than twice as much as C by its atomic $f_I(q)$. The opposite occurs in ND, where C is weighted more than Si, having a ND coherent length ($b_C = 6.65$ fm) sensibly larger than that of Si ($b_{Si} = 4.15$ fm). Furthermore, the presence of H can be detected directly in neutron but not in XR diffraction experiments. Therefore, a total DF obtained by ND measurements can provide information complementary to those coming from J_{XR}. In Fig. 2 (lower panel) we plotted the DF $J_N(R)$ (thick line) defined as

$$J_N(R) = 4\pi R^2 n \frac{\sum_{I,J} b_I b_J c_I c_J g_{IJ}(R)}{\sum_{I,J} b_I b_J c_I c_J}. \quad (3)$$

In order to allow a direct comparison with the output of ND experiments, in Fig. 2 the same data convoluted with the experimental resolution function[25] corresponding to $q_{max} = 30$ Å^{-1} (thin line) are also shown. It is seen that C-H and C-C bonds give rise to prominent features in J_N before the most intense peak coming from Si-C first neighbors. The deep minimum around $R = 2.4$ Å is mainly due to Si-H and C-H second neighbors (see Table I), since neutrons are backscattered by H ($b_H = -3.73$ fm). The broad maximum at about 3 Å comes instead from Si-C, Si-Si, and C-C second neighbors.

In summary, we have presented *ab initio* MD simulations of the structural properties of a-$Si_{0.5}C_{0.5}$:H at 20% H content. The structure of the alloy turns out to be a complex network composed of homonuclear and heteronuclear bonds, similar to that found in the simulation of pure a-Si-C,[14] but with a larger proportion of Si-C bonds. The presence of H favors the formation of a tetrahedral network and thus enhances the chemical order in the material. Analyses of the different bonding configurations have revealed that hydrogenated C forms tetrahedral units, whereas C not bonded to H gives rise to sites with bonding intermediate between sp^2 and sp^3. H bound to Si does not only passivate dangling bonds but originates several different bonding configurations: we could identify strong H-Si bonds, with lengths similar to those of the silane molecule [SiH_4] and weaker bonds, characterized by longer distances. These occurrences of weak bonds can be correlated with the occurrence of fivefold coordinated Si atoms.

ACKNOWLEDGMENTS

It is a pleasure to thank G. Ciccotti for useful discussions. We acknowledge support from Italian CNR under "Progetto finalizzato sistemi informatici e calcolo parallelo" (F.F.) and from the Swiss National Science Foundation under Grants No. 20-30272.90 and 21-31144.91 (G.G.). Calculations were carried out at the IDRIS Computational Centre in Orsay.

* Present address: Laboratoire de Physique des Solides (Unité Associé au CNRS), Bâtiment 510, Université Paris-Sud, 91405 Orsay CEDEX, France.

[1] For a recent review, see, e.g., J. Robertson, Philos. Mag. B **66**, 615 (1992).
[2] A. H. Mahan, B. von Roedern, D. L. Williamson, and A. Madan, J. Appl. Phys. **57**, 2717 (1985).
[3] D. R. McKenzie, G. B. Smith, and Z. Q. Liu, Phys. Rev. B **37**, 8875 (1988).
[4] P. J. R. Honeybone *et al.*, J. Non-Cryst. Solids **169**, 54 (1994).
[5] A. Tabata *et al.*, J. Appl. Phys. D **23**, 316 (1990).
[6] G. H. Bauer, H. D. Mohring, G. Bilger, and A. Eicke, J. Non-Cryst. Solids **77/78**, 873 (1985).
[7] N. Saito *et al.*, Philos. Mag. B **52**, 987 (1985).
[8] S. L. Wang and F. Evangelisti (unpublished); F. Evangelisti, J. Non-Cryst. Solids **164/166**, 1009 (1993).
[9] A. M. Haghiri-Gosnet *et al.*, Microel. Eng. **17**, 215 (1992).
[10] S. Pascarelli, F. Boscherini, S. Mobilio, and F. Evangelisti, Phys. Rev. B **45**, 1650 (1992).
[11] R. Car and M. Parrinello, Phys. Rev. Lett. **55**, 2471 (1985).
[12] F. Buda, G. L. Chiarotti, R. Car, and M. Parrinello, Phys. Rev. B **44**, 5908 (1991); I. Stich, R. Car, and M. Parrinello, Phys. Rev. B **44**, 11 092 (1991).
[13] S. Iarlori, G. Galli, and O. Martini, Phys. Rev. B **49**, 7060 (1994); G. Galli, R. Martin, R. Car, and M. Parrinello, Phys. Rev. Lett. **62**, 555 (1989); Phys. Rev. B **42**, 7470 (1990).
[14] F. Finocchi, G. Galli, M. Parrinello, and C. M. Bertoni, Phys. Rev. Lett. **68**, 3044 (1992).
[15] A. Sproul, D. R. McKenzie, and D. J. H. Cockayne, Philos. Mag. B **54**, 113 (1986).
[16] G. B. Bachelet, D. R. Hamann, and M. Schlüter, Phys. Rev. B **26**, 4199 (1982).
[17] A thorough account of these calculations will be given in a longer report [F. Finocchi and G. Galli (to be published)]; as indicative examples it is worth mentioning that the C-H and Si-H distances in CH_4 and SiH_4 are overestimated by 1.5% and 1%, respectively, and that the errors on the vibrational frequencies of these molecules are at most 4%. The lattice constant of c-SiC is overestimated by 0.5% by our calculation, and its bulk modulus underestimated by 4%. The formation energy of c-SiC with respect to elemental crystals is calculated to be 0.24 eV/atom, to be

compared with the local density approximation results of K. J. Chang and M. L. Cohen [Phys. Rev. B **35**, 8196 (1987)], 0.28 eV/atom, and with the experimental value of 0.33 eV/atom.

[18] $X^{(n)}$-Y denotes n-fold coordinated X sites, (X=C, Si), where one of the neighbors belongs to species Y (Y=C, Si, or H).

[19] M. A. Petrich, K. K. Gleason, and J. A. Reimer, Phys. Rev. B **36**, 9722 (1987).

[20] G. Della Mea *et al.*, J. Non-Cryst. Solids **137/138**, 95 (1991).

[21] H. J. Schliwinski *et al.*, Mater. Sci. Eng. B **11**, 73 (1992).

[22] R. A. Street and K. Winer, Phys. Rev. B **40**, 6236 (1989).

[23] In general, the peaks of $g_{IJ}(R)$ are not symmetric and cannot be easily approximated by a Gaussian; therefore, their positions differ by several hundredths of an Å from the average bond distance between I and J, computed over the whole simulation run by taking as cutoff distances the minima of the $g_{IJ}(R)$.

[24] C. Meneghini *et al.*, J. Non-Cryst. Solids **137/138**, 75 (1991).

[25] G. Etherington *et al.*, J. Non-Cryst. Solids **48**, 265 (1982).